



HAL
open science

Pushing the limits of native MS: Online SEC-native MS for structural biology applications

Evolène Deslignière, Marie Ley, Maxime Bourguet, Anthony Ehkirch, Thomas Botzanowski, Stéphane Erb, Oscar Hernandez-Alba, Sarah Cianférani

► To cite this version:

Evolène Deslignière, Marie Ley, Maxime Bourguet, Anthony Ehkirch, Thomas Botzanowski, et al.. Pushing the limits of native MS: Online SEC-native MS for structural biology applications. International Journal of Mass Spectrometry, 2021, 461, pp.116502. 10.1016/j.ijms.2020.116502 . hal-03160756

HAL Id: hal-03160756

<https://hal.science/hal-03160756>

Submitted on 12 Oct 2021

HAL is a multi-disciplinary open access archive for the deposit and dissemination of scientific research documents, whether they are published or not. The documents may come from teaching and research institutions in France or abroad, or from public or private research centers.

L'archive ouverte pluridisciplinaire **HAL**, est destinée au dépôt et à la diffusion de documents scientifiques de niveau recherche, publiés ou non, émanant des établissements d'enseignement et de recherche français ou étrangers, des laboratoires publics ou privés.

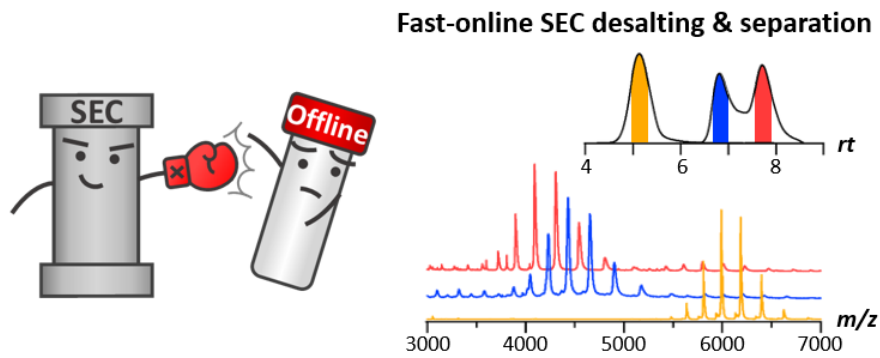
Pushing the limits of native MS: Online SEC-native MS for structural biology applications

Evolène Deslignière¹, Marie Ley¹, Maxime Bourguet¹, Anthony Ehkirch¹, Thomas Botzanowski¹, Stéphane Erb¹, Oscar Hernandez-Alba¹, Sarah Cianférani^{1*}

¹Laboratoire de Spectrométrie de Masse BioOrganique, Université de Strasbourg, CNRS, IPHC UMR 7178, 67000 Strasbourg, France

*Corresponding author: Sarah Cianférani. Email: sarah.cianferani@unistra.fr

Abstract



Native mass spectrometry (nMS) is now widely applied to investigate non-covalently assembled biomolecule complexes. nMS requires the use of near-neutral pH and volatile buffers to preserve the native state of proteins. However, buffer exchange into nMS-compatible solvent is usually performed manually, which results in a time-consuming and tedious process, thus appearing as a major drawback for nMS analysis. Conversely, online coupling of size exclusion chromatography (SEC) to nMS affords a fast-automated and improved desalting, but also provides an additional dimension of separation for complex protein mixtures. We illustrate here the benefits of SEC-nMS compared to manual offline desalting for the characterization of a wide variety of biological systems, ranging from multiprotein assemblies, protein–ligands and protein–nucleic acid complexes, to proteins in a detergent environment. We then highlight the potential of the coupling to further integrate ion mobility while preserving the native conformations of proteins, allowing for rapid collision cross section measurement and even collision-induced unfolding experiments. Finally, we show that online SEC coupling can also serve as the basis for multidimensional non-denaturing liquid chromatography (LC) workflows, with the SEC acting as a fast desalting device, helping to achieve first dimension LC separation in optimal chromatographic conditions while being compatible with further nMS analysis.

Keywords

Size Exclusion Chromatography, Native Mass Spectrometry, Ion Mobility, LC-MS

Introduction

Native MS (nMS) remained for a long time the prerogative of few academic expert laboratories. The recent growing interest of biopharma companies for this methodology, especially for the characterization of therapeutic proteins like monoclonal antibodies (mAbs), prompted manufacturers to develop new instrumentations adapted to biopharma specific requirements, from sample preparation to data acquisition and treatment.

nMS was first introduced in the early 90s by the groups of Katta&Chait and Henion for the analyses of myoglobin¹ and kinase/substrate² complexes. The validity of gas phase nMS to conclude about solution binding stoichiometries and even more for affinities was for a long time a question of heated debates: “Do gas phase native MS spectra really reflect solution phase behavior?”; “Are gas phase data reliable to extrapolate solution phase behavior?”. Major advances in studying macromolecular interaction by nMS have been performed by the groups of Carol Robinson and Albert Heck, and helped converting early skepticism into competence and consistency of practical use of nMS. nMS provides unambiguous determination of subunit stoichiometry, the most straightforward and important application of nMS, on a variety of biological assemblies ranging from multiprotein, e.g. transthyretin, retinol binding³, GroEL⁴, or HSP⁵, to protein–ligand and protein–nucleic acid assemblies, including RNA editing complexes like the CRISPR-Cas systems⁶, RNA polymerase II⁷, and ribonucleoparticles⁸. Applications of nMS also encompass highly complex membrane proteins such as TRP channels⁹, GPCR¹⁰ or ABC transporters¹¹, and binding of lipids¹² or other small molecules¹³ to membranes for which high resolution instrumentations is a real breakthrough. Even MegaDaltons ribosomes¹⁴, hemocyanines¹⁵, COP9 signalosome¹⁶, dynactin complex¹⁷ and virus particles with masses up to 18 MDa¹⁸ can be measured by nMS.

From 2005, hyphenation of ion mobility (IM) spectrometry to native MS added a new dimension of gas-phase data interpretation, affording conformational characterization along with stoichiometry determination. Ruotolo first described a new type of instrumentation combining nMS and ion mobility (nIM-MS) and demonstrated that the overall topology of a ring-shaped protein complex could be retained in the gas phase¹⁹. More advanced strategies combining gas phase activation to nIM-MS, termed collision-induced unfolding (CIU), allow assessing differential gas phase unfolding behavior of proteins. Overall, nIM-MS demonstrated that most solution structures are retained into the gas phase^{19,20}.

However, despite all those technological breakthroughs, nMS was still poorly implemented in industrial environments in 2015, mostly due to its lack of automation. Indeed, prior to nMS, sample preparation consisting of buffer exchange has to be performed manually, hampering throughput necessary in companies. nMS analyses have to be performed in a volatile buffer, compatible with electrospray ionization and able to preserve weak noncovalent complex assemblies in solution²¹. Ammonium buffers are thus classically used for nMS analyses. Sample preparation usually consists of manual buffer exchange, or desalting, into ammonium acetate using a variety of devices such as gel filtration devices, microconcentrators or dialysis units, a step which is quite time-consuming, labor intensive and in some cases delicate. It can also lead to alteration of the sample, including aggregation, precipitation, or chemical modifications. Hence, this manual buffer exchange process appears as a major drawback for nMS analysis automation and throughput increase. The size exclusion chromatography (SEC), for which separation is based on the differences in hydrodynamic volumes, is achieved through a column packed with particles having precise pore sizes, which makes SEC interesting for fast buffer exchange, that is, separation of small nonvolatile salt molecules from protein species, and/or separation of high versus low mass proteins contained in a mixture.

Even if already suggested in early 2003 by Cavanagh et al. using self-packed gel filtration cartridges²² and few years later by Waitt et al. in 2008 with commercial SEC columns²³, the online coupling of SEC to nMS only became reality five years later for reference proteins^{24, 25}, soluble protein/protein complexes²⁶ and biotherapeutics²⁷⁻³² analysis. Several reasons may account for the delay between first experiments and its effective wider application, among which: (i) the fact that older generation of MS instruments were not sufficiently tolerant to high salt contents necessary for nMS analysis, even volatile salts such as ammonium acetate, (ii) the lack of chemical inertness of SEC columns leading to poor peak shapes with volatile salts, and (iii) the amount of starting biomaterial. SEC afforded first a way to automate nMS experiments providing rapid assessment of proteins and complexes integrity of large numbers of samples, using small sample quantities (between 2 and 5 μg).

The benefit of SEC-nMS has been broadly documented by our group^{27, 28, 33} and others²⁹⁻³² for therapeutic proteins characterization, more particularly for mAb-based product analysis. In the present work, we aim at widening the scope of SEC-nMS use for different systems of interest we had in the lab. After first presenting the SEC-nMS technical parameters to be optimized for each system, several examples will serve to discuss benefits but also limitations of online SEC-nMS. We then show the efficiency of the coupling to further integrate ion mobility for fast collision cross section measurement and collision-induced unfolding experiments. Lastly, we demonstrate how online SEC coupling can also be used as the basis to develop multidimensional non-denaturing liquid chromatography (LC) setups, with the SEC column acting as a fast desalting device, helping to achieve first dimension LC separation in optimal chromatographic conditions while being compatible with nMS analysis.

1. Practical aspects and advantages of online SEC-nMS

Columns – Several types of SEC columns are currently available on the market from different manufacturers for the analysis of proteins and macromolecular complexes. They offer a wide variety in terms of column dimensions, stationary phase chemistry, particle sizes and porosities. More particularly, the development of sub-3 μm (from 1.7 to 2.7 μm) particle size SEC columns, also considered as the new generation SEC columns, allowed to improve separation and column efficiency while significantly reducing the analysis time between three- and five-fold with runs performed in dozens of minutes³⁴ (Figure S1). As expected, the highest resolution is achieved with the lowest SEC particle size (< 2 μm). SEC columns are also available with different lengths, from 30 to 300 mm, that will affect the separation of the different protein populations and their nMS signal.

Mobile phase – Among the different parameters that have to be optimized to perform online SEC-nMS, the ionic strength and the pH of the mobile phase are critical to maintain the native conformation of the proteins. Those parameters mainly depend on the nature of the analyte and are the same as for offline nMS. SEC-nMS experiments can be performed with ammonium acetate, bicarbonate or formate mobile phases. Ventouri et al. conducted in-depth investigation on the ability of SEC-nMS to preserve the native fold of reference proteins depending on the nature, pH and ionic strength of the solvent³⁵. Ammonium acetate was more effective to retain the native protein conformation under near-physiological pH conditions, although adsorption and peak tailing could be observed especially at lower ionic strength, which was also reported for mAb analysis³⁶. Ammonium bicarbonate and formate may lead to higher fractions of denatured populations^{35, 37}; however, the presence and level of denatured species depend on the analyte, and need to be evaluated for other types of proteins.

Online SEC-nMS for high throughput online buffer exchange – For online desalting purposes, the focus will be on using short SEC columns (30 – 50 mm), as increased runtimes will be obtained with longer columns²⁴. A compromise between short time of analysis, keeping efficient separation of low molecular weight non-volatile salts and proteins, limited protein adsorption on the stationary phase and acceptable MS intensities has to be found. Several short new-generation SEC columns between 30 and 50 mm are currently available from different manufacturers (ThermoFisher, Waters, Agilent, Phenomenex, etc.). Online SEC-nMS analysis of therapeutic mAbs could be successfully achieved with any of those columns, but in our hands, Waters BEH200 30 mm and Agilent AdvanceBio SEC 50 mm afford the best compromise for therapeutic protein analysis and are used at first line. However, protein adsorption could be different for other types of proteins. The flowrate also plays a critical role on SEC-nMS data: even if flowrates ranging between 100 and 250 $\mu\text{L}/\text{min}$ can be used, lower elution flowrates (100 $\mu\text{L}/\text{min}$) usually provide increased nMS signal-to-noise ratio (Figure S2) and are thus better suited²⁸. To conclude, for high throughput purposes resulting in < 5 min runs, the shortest columns (30 – 50 mm) with smallest particle size (< 3 μm) should be preferentially selected (Figure S1).

SEC is particularly well-adapted to perform online buffer exchange for proteins for which manual desalting may induce the precipitation of the sample or does not completely remove the non-volatile salts of the original buffer. The benefits of online SEC-nMS is clearly exemplified with a mAb-RNA conjugate (Figure 1A). After 6 cycles of Vivaspin, only minor noisy MS signal that could correspond to the mAb-RNA conjugate is observed in the m/z range 6000 – 7500 (Figure 1 A1), avoiding any mass calculation and determination of RNA distribution and binding stoichiometry. Conversely, SEC-nMS analysis affords efficient sample desalting and detection of several species with accurate mass measurements (Figure 1 A2).

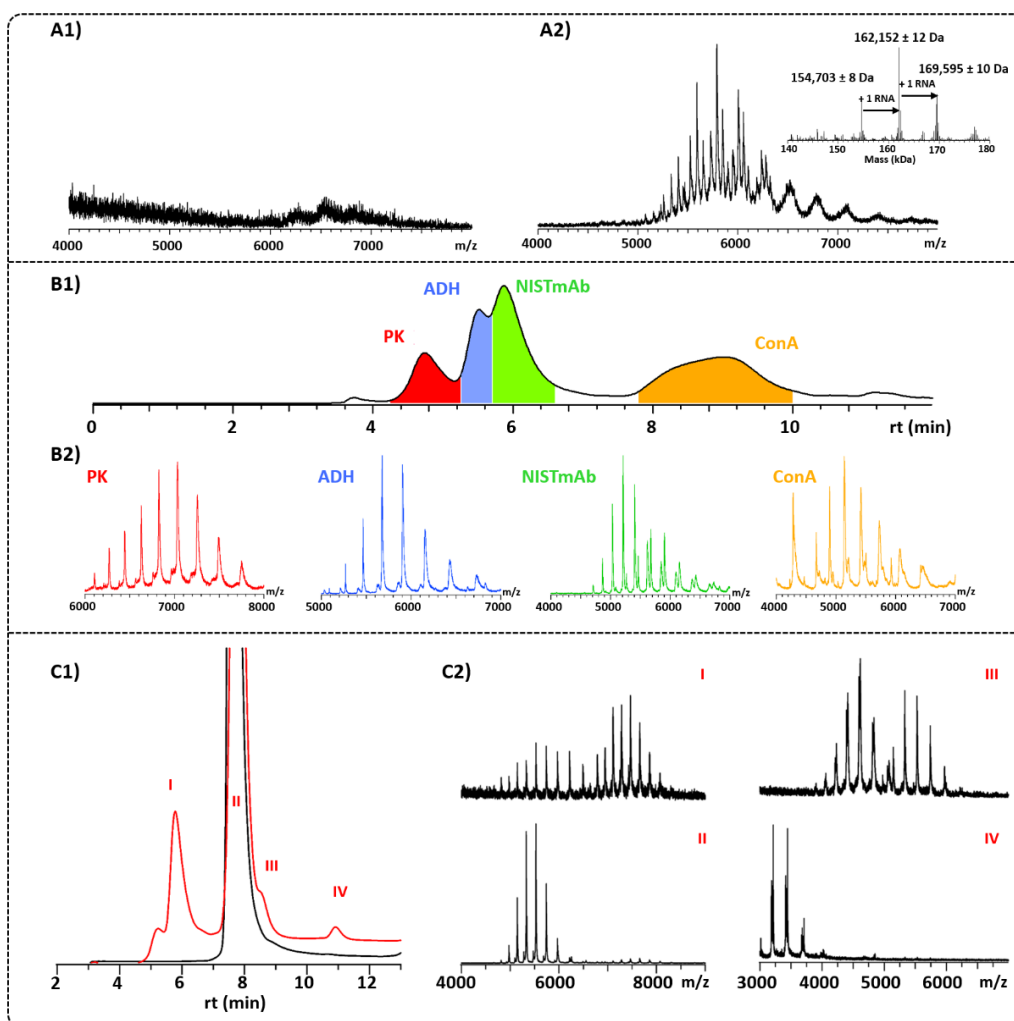


Figure 1. SEC-nMS for efficient desalting and improved protein separation. Native mass spectrum of mAb-RNA conjugate obtained with (A1) manual desalting and (A2) online SEC-nMS. (B1) Chromatographic separation and (B2) corresponding native mass spectra of a mixture of four reference proteins (PK, ADH, ConA, and deglycosylated NISTmAb) obtained with a 300 mm SEC column (Waters BEH125). (C1) Chromatogram of nonstressed (black line) and thermal-stressed (red line) bevacizumab. (C2) Native mass spectra corresponding to the high molecular weight species (HMWS) and low molecular weight species (LMWS) of bevacizumab after thermal stress.

Online SEC-nMS for improved protein separation – One of the main issues in analyzing complex protein mixtures is the difference in ionization efficiencies of the constituents that might lead to an overwhelming MS signal of the protein with the highest ionization efficiency, and very minor signals detected in the noise of the native mass spectrum. In such cases where several species may hamper the detection of each other, SEC-nMS might be an interesting alternative to simultaneously afford sample desalting and separation of proteins based on their hydrodynamic volume, leading to an easier and straightforward native mass spectra interpretation. For separation purposes, longer columns (150 or 300 mm) with enhanced chromatographic separation capabilities but also longer run times will be preferred²⁸. A mixture composed of four reference proteins, ConA, ADH, NISTmAb and PK, was analyzed with an Acquity BEH200 (4.6 x 30 mm, 1.7 μ m) column (Figure 1B). Reference proteins were efficiently separated in the chromatographic dimension as depicted in figure 1 B1. Only NISTmAb and ADH show two overlapping peaks since they exhibit very similar hydrodynamic volumes. In this case, the mass spectra associated with both peaks allowed the identification of both proteins (Figure 1 B2).

Thereby proteins with different sizes can be separated with long SEC columns (300 mm) avoiding ionization competitions between the analytes, which enables a more reliable identification and quantification of different populations.

Another application of SEC-based protein separation is the separation and quantification of LMWS and HMWS³⁸ in forced degraded studies. When using nMS as a standalone technique, the relative quantification of protein size variants can be misleading due to the modification of the intensity of the different oligomers that may arise at the interface of the mass spectrometer as a consequence of the ionization process (disruption of noncovalent bonds, formation of nonspecific interactions, ionization competition between HMWS and LMWS). Upon thermal stress, the intensity of HMWS and LMWS increases compared to the non-stressed mAb sample (Figure 1 C1), and the relative quantitation of each population can be assessed based on the areas of chromatographic peaks. However, the relative quantification of HMWS and LMWS significantly varies when using nMS as standalone technique (Figure S3). In this case, the relative intensity of the dimer is estimated to 21.5 % (Figure S3A) compared to 14.5 % (Figure S3B) with online SEC-nMS data, which corresponds to a variation of 50 %. These differences stem on the formation of nonspecific HMWS in the interface of the mass spectrometer during the ionization process compared to nanoESI-nMS. For this reason, online SEC-nMS is particularly well-suited to assess protein stability through force degraded studies by comparing the relative intensity of the size variant populations. Online SEC-nMS enables an efficient separation, a more reliable quantification and a simultaneous identification of high- and low-molecular species to afford a precise characterization of protein degradation.

Sensitivity of SEC-nMS – Overall, SEC-nMS coupling often requires larger amount of sample compared to nanoESI-nMS. Even though the sensitivity of the technique depends on several factors such as the ionization efficiency of the analyte or the type of mass spectrometer used, injected material can vary from 2 to 5 µg. However, mass spectra with a suitable S/N ratio can be obtained with less material. The limit of detection of our online SEC coupled to a Synapt-G2 HDMS mass spectrometer with glycosylated pertuzumab was established to 1 µg (Figure S4), where the S/N ratio (80) and the resolution of the MS peaks ($R_s @m/z 5290 = 587$) allow an accurate mass measurement and assignment of all mAb populations. Lower amounts could be injected in other SEC-nMS setups²⁶, nevertheless 1 µg of loaded mAb offers an adequate trade-off between the amount of sample and mass spectrum quality.

Main SEC-nMS drawbacks – The use of volatile salts in the mobile phase of SEC-nMS systems may induce further interactions with the stationary phase of the column, leading to the coelution of different protein populations³⁶ or providing some discrepancies between the elution volumes and the hydrodynamic volume of the oligomers²⁴. Since SEC separation is based on the hydrodynamic volume, only proteins with different sizes will be efficiently separated, otherwise, only coeluting or partially resolved chromatographic peaks will be obtained with this kind of chromatography. In addition to possible interactions with the stationary phase, sample dilution in the mobile phase will occur due to diffusion in the column, which may also dissociate unstable and/or low affinity complexes.

Normally, nMS is performed in the nanoESI regime to reduce the amount of injected sample. Conversely, SEC-nMS experiments are performed in ESI ionization mode and thus require higher amounts of starting material. Upon addition of SEC dimension, the flowrate is increased significantly (between 100 and 300 µL/min) implying the use of higher desolvation gas and source temperatures to improve solvent evaporation and hence, enhance nMS data. The latter parameter has been recently

reported in the literature to have an impact on mAb gas-phase energetics by increasing the internal energy of the ions³³. These results suggest that source temperatures, and desolvation gas temperatures, need to be carefully adjusted to avoid further source activation and/or fragmentation. In spite of these potential drawbacks, this review illustrates numerous examples where SEC in combination with nMS has been used to provide further insights into the characterization of therapeutic proteins and macromolecular complexes, and hence, showing the suitability of this coupling for structural biology.

2. SEC-nMS is suitable for a variety of noncovalent complexes analyses

Protein/ligand and protein/metal interactions – SEC-nMS can help to probe noncovalent interactions between proteins and small molecules. nMS has been reported for high-throughput screening of ligands libraries against enzymes or receptors, the latter being extensively applied in drug discovery. nMS has already been reported as a straightforward, fast and reproducible method to detect ligand binding to specific targets, but also to determine binding affinity, stoichiometry and specificity³⁹, thus appearing as an attractive technique to complement more common approaches including nuclear magnetic resonance, or surface plasmon resonance⁴⁰. However, the use of SEC coupled to nMS has been scarcely reported in literature.

Quinn's group has presented an online SEC-ESI-FTICR-MS approach to detect protein-ligand noncovalent complexes and to screen natural product extracts⁴¹. A second study details the technical developments and optimizations of SEC-nMS as a robust, quantitative, and automated platform to measure affinities of noncovalent protein–small molecule interactions on an Orbitrap instrument using indoleamine 2,3-dioxygenase 1 (IDO1), a catabolic enzyme, and inhibitory ligands as case study⁴². The scarce use of SEC coupled to nMS for protein–ligand screening may be explained by the risk of cross contamination, as high affinity ligand absorption on the SEC column may prevent further detection of binding of a lower affinity molecule to the target protein. Alternative nanoESI microfluidic devices, e.g. the Triversa Nanomate from Advion, have been developed, combining capabilities of sample preparation such as ligand addition to the protein and temperature-controlled incubation to reproducible nanoESI injection and nMS analysis⁴³. Benefits of such systems is that using individual nozzles for each ligand/mixture of ligand prevents from cross contamination of capillaries or columns. SEC-nMS can also be of interest to investigate protein–metal interactions, as reported by Jia et al. for [2Fe-2S] cluster-bridged complexes, for which offline nanoESI-nMS failed to detect cluster-bound species⁴⁴. As iron-sulfur clusters are sensitive to oxygen, SEC-nMS helps to minimize the possibility to oxidize unstable analytes due to reduced sample preparation and shorter time of analysis. Here, SEC-nMS performed under inert atmosphere (injection valve, sample syringe and samples flushed with argon) revealed the presence of a GLRX5 homodimer with one [2Fe-2S] cluster. This setup also allowed to monitor cluster transfer reactions to get better insight into intermediate [2Fe-2S] species, proving that SEC-nMS can be used as a robust and fast technique to elucidate both the cluster and protein components.

Protein/protein interactions – SEC is commonly used to investigate protein oligomerization state or more generally the distribution of size variants of a sample⁴⁵. It is also often the last step of protein/complex purification. We thus performed systematic comparison of manual desalting followed by nMS analysis versus online SEC-nMS for different systems of increasing complexity. The first example relies on the oligomeric state assessment of a homo-oligomeric soluble protein, PRMT2, a

member of the protein arginine methyltransferase family that has diverse roles in transcriptional regulation⁴⁶. Figure 2 A1-2 presents the nMS mass spectra obtained after manual desalting (two cycles of Zeba 7 kDa, AcONH₄ 500 mM, pH 7.0) or SEC- nMS analysis of mouse PRMT2. Except differences in the charge state distributions (CSD) due to the use of nanoESI versus ESI, similar mass spectra were obtained, highlighting the presence of two CSDs, a minor one with a mass of $50\,726 \pm 1$ Da corresponding to monomeric (PRMT2)₁ and a major one of $101\,517 \pm 3$ Da corresponding to dimeric (PRMT2)₂. The PRMT2 example shows the potential of SEC-nMS to preserve the oligomerization state of a protein known as dimeric. Additionally, SEC-nMS ensures the spray stability at high concentration of AcONH₄ (500 mM) contrary to nanoESI-nMS.

Benefits of SEC is further illustrated on the multiprotein P1-P2 complex system. The nMS spectrum (Figure 2 B1) obtained after manual desalting is highly complex and presents several CSDs. The first one between m/z 1000 and 2500 corresponds to partially unfolded monomeric P1 and P2; from m/z 2500 to 3500, the most intense CSDs correspond to folded monomeric P1 and P2 species; finally, in the m/z range 3700 – 5000, minor signals of homo/heterodimers are detected. Conversely, online SEC-nMS analysis of an equimolar mixture of P1 and P2 (100 μ M of each, 1-hour room temperature incubation) revealed three partially resolved chromatographic peaks (inset, Figure 2 B2). The most intense chromatographic peak corresponds to (P1)₂ homodimers ($64\,914 \pm 1$ Da), followed by a second peak with a mass of $59\,973 \pm 2$ Da in agreement with a 1:1 stoichiometric (P1)₁(P2)₁ heterodimer (Figure 2 B2) and finally a peak at 7.8 min corresponding to (P2)₂ homodimers ($55\,030 \pm 1$ Da). This example illustrates the benefits of using SEC separation capabilities (even if partial) to compensate for overlapping CSDs, “polishing” the differences in ionization efficiencies of monomers and dimers and resulting in better quality nMS spectra.

Finally, SEC-nMS is also adapted to the characterization of HMW complexes (> 100 kDa). Yeast Rvb1 and Rvb2 are involved in various cellular processes ranging from ribonucleoprotein complex biogenesis to chromatin remodeling⁴⁷. Rvbs predominantly assemble into hexameric rings > 300 kDa⁴⁷, and are generally purified with buffers containing ADP, which helps to maintain the integrity of the hexamers⁴⁸. The nMS spectrum obtained after manual desalting (Zeba 7 kDa, AcONH₄ 150 mM, pH 7.5) shows that monomers are mainly detected, and only low intensity signals with $S/N = 5$ are observed for hexamers, suggesting that complex stabilization *via* ADP was not retained with manual buffer exchange (Figure 2 C1). Online SEC-nMS experiments performed using 150 mM ACONH₄ as mobile phase demonstrate the potential of the coupling to preserve noncovalent interactions within the hexameric ring of Rvbs, while improving the resolution ($R_s @m/z\ 8106 = 811$) and the intensity of the signal (71 S/N) (Figure 2 C2). SEC-nMS highlights the presence of two populations of hexamers bearing 5 and 6 ADP respectively, the predominant one being bound to 6 ADP ($307\,973 \pm 8$ Da).

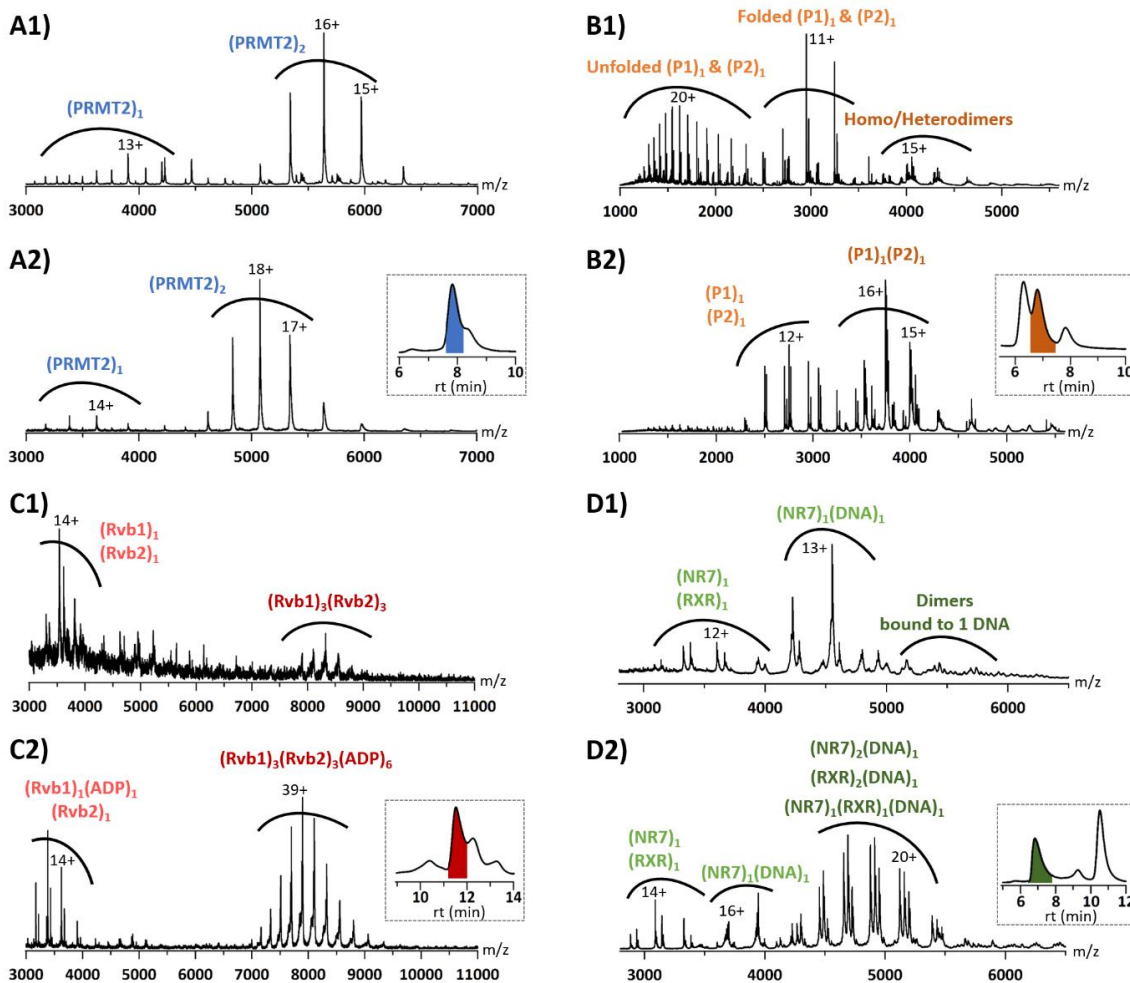


Figure 2. Offline nanoESI-nMS (A1, B1, C1, D1) versus online SEC-nMS experiments (A2, B2, C2, D2) with corresponding SEC-UV chromatograms at 280 nm depicted in insets. Native mass spectra of (A) PRMT2, (B) an equimolar 1:1 P1:P2 mixture, (C) HMW Rvbs complexes, and (D) nuclear receptors RXR and NR7 bound to DNA.

Protein/nucleic acid interactions – For protein-nucleic acid complexes with either RNA or DNA, an additional challenge has to be faced related to the presence of cations associated to oligonucleotide binding which in turn often leads to low quality nMS signals with broad peaks, low mass spectral resolution, and difficult data interpretation. Interactions of nuclear receptors with their cognate DNA response elements serve to illustrate this point. NR7 and RXR are transcription factors that can bind a variety of ligands which can further interact with specific DNA sequences, known as response elements, either as monomers or hetero/homodimers. nMS is often used to assess the binding stoichiometry of complexes involving nuclear receptors^{49, 50}. In this example, nMS was employed to uncover the dimerization properties of NR7 and RXR upon DNA binding. The nMS spectrum obtained after manual buffer exchange (Zeba 7 kDa, AcONH₄ 150 mM, pH 8.0) followed by complex reconstitution of NR7, RXR and DNA (1 hour at 4 °C) reveals that the most intense CSD corresponds to the binding of one monomer of NR7 to a DNA fragment of 15 940 Da (Figure 2 D1). Low intensity signals corresponding to HMWS are also observed in the 5300 – 5800 *m/z* region, but do not allow accurate mass measurements and proper mass-based identification. Conversely, the online SEC-nMS analysis (150 mM ACONH₄ pH 8.0 after the complex reconstitution) exhibits very different results. The first chromatographic peak at 6.8 min reveals the coexistence of different dimers each bound to one DNA fragment: (NR7)₂ homodimers (102 411 ± 1 Da), (RXR)₂ homodimers (103 944 ± 2 Da) and 1:1

(NR7)₁(RXR)₁ heterodimers (103 177 ± 2 Da) (Figure 2 D2). The second chromatographic peak at 9.3 min corresponds to the binding of NR7 to DNA as a monomer (59 178 ± 2 Da), while the last peak at 10.5 min shows the presence of isolated DNA species. Thus, online SEC-nMS allowed to unambiguously characterize the binding combinations between NR7, RXR and the DNA, highlighting the fact that these NRs predominantly bind DNA as dimers. Here, these results emphasize the potential of SEC-nMS to preserve and transmit heterogeneous protein–nucleic acids complexes.

SEC-nMS for proteins in a detergent environment – Membrane protein analysis by nMS is still challenging as it needs to be performed in a detergent environment. Online SEC-nMS can be applied also in presence of detergents, as depicted with the determination of the oligomeric species constituting amyloid-beta (A β) pores that form in the membrane of neurons to explain neurotoxicity in Alzheimer's disease⁵¹. Figure 3A presents the nMS spectrum of the β -sheet pore-forming (β PFO) A β (1-42) after manual desalting in C8E5 detergent. Several species ranging from monomers of high intensity to possible octamers of very low intensity were detected, precluding to conclude about the main species present in solution. To circumvent these limitations, SEC-nMS was performed in 200 mM ammonium bicarbonate pH 9.0 with 14.2 mM C8E5 detergent as mobile phase to benefit from SEC separation capabilities. SEC-nMS analysis of β PFO_{A β (1-42)} resulted in two partially separated chromatographic peaks: the peak at 6.3 min corresponds to octamers (36 114 ± 1 Da) due to the presence of intense 9+ and 7+ ions of the octamer, while the peak at 7.0 min could be attributed to tetramers (18 056 ± 1 Da) (Figure 3B). Comparison of SEC-nMS analysis of low versus high concentrations of A β (1-42) revealed that the former was enriched in A β (1-42) tetramers and the latter in octamers (inset, Figure 3B)⁵¹. SEC-nMS presented a unique opportunity to establish the stoichiometry of the potentially distinct oligomer species of β PFO_{A β (1-42)}, revealing that the main species present in the β PFO_{A β (1-42)} sample were A β (1-42) tetramers and octamers⁵¹. In addition, since no charge states specific for other oligomer stoichiometries between tetramers and octamers were detected, these results suggested that tetramers were the building block for octamer formation. Overall, SEC-nMS appears promising to characterize membrane proteins in detergent environments, however, further developments are still necessary, as high amounts of non-volatile detergents are required. Besides, higher flowrates used in online SEC-nMS compared to nanoESI-nMS may reduce MS sensitivity, and dissociation of unstable membrane protein complexes may occur⁵².

3. Hyphenation of ion mobility to SEC-nMS for conformational characterization of protein and protein complexes

nIM-MS is now broadly used in structural biology to study the gas-phase conformations of protein and their noncovalent complexes^{53, 54}. IM separates ions based on their size, shape and charge under the influence of an electric field as they drift through an inert buffer gas in the mobility cell. Drift times can be further converted into rotationally averaged collision cross sections (CCS), which correspond to projected areas of ions. IM affords an additional level of gas-phase characterization, and can help not only to separate isomers but also to examine conformational changes upon complex formation. Hence, the hyphenation of SEC to nIM-MS, which was first reported by Van der Rest et al.²⁴, is of main interest to rapidly gain further insight into proteins conformations.

SEC-nIM-MS for spectrum cleaning and unambiguous CSDs attribution of oligomers – When several oligomerization states of a protein coexist, unambiguous peak assignment may not be achieved with SEC-nMS due to both low intensities or lack of isotopic resolution for higher oligomeric states. The

benefit of SEC-nIM-MS for the separation of isobaric species along with unambiguous peak attribution of oligomers is clearly evidenced in the case of A β (1-42)s, which form monomers, dimers, trimers, tetramers and octamers⁵¹. For instance, mass spectra obtained with SEC-nMS (Figure 3B) exhibit a peak at m/z 3010 that could correspond to either dimeric ($z = 3+$), tetrameric ($z = 6+$) or octameric ($z = 12+$) species. With the addition of IM, the arrival time distribution (ATD) corresponding to m/z 3010 highlights the presence of two different populations at 8.55 and 12.01 ms (inset, Figure 3C) which were identified as tetramers ($z = 6+$) and dimers ($z = 3+$), respectively. Since ions belonging to the same series are diagonally aligned on bidimensional drift time vs m/z plots, tetrameric 5+ ions and octameric 8+ ions could also be assigned (Figure 3C). This example demonstrates the potential of SEC-nIM-MS to assess the coexistence of oligomeric states for identical m/z while ensuring unambiguous CSDs attributions.

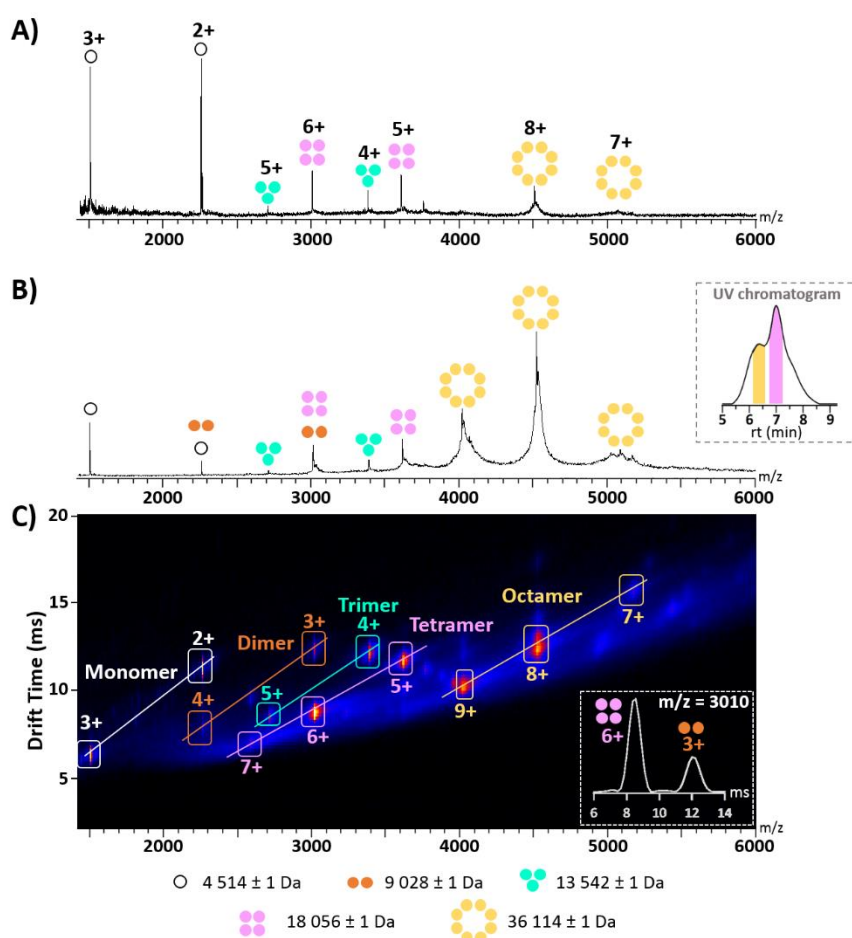


Figure 3. nanoESI- and SEC-ESI- nIM-MS experiments of A β (1-42). (A) Native nanoESI mass spectrum obtained after manual desalting. (B) Native SEC-ESI mass spectrum corresponding to the chromatographic peak of the octamer (yellow slice of UV chromatogram shown in inset). Species were identified as monomers (white), dimers (orange), trimers (green), tetramers (pink) and octamers (yellow). (C) 2D SEC-nIM-MS Driftscope plot with charge state distributions of the different oligomers. The extracted ATD at m/z 3010 is shown in inset.

SEC-nIM-MS for high-throughput CCS measurements of biotherapeutics – While the use of nIM-MS is commonplace in academic research laboratories, it remains scarce in biopharmaceutical companies. Although nIM-MS has already proven valuable to characterize biotherapeutic proteins such as mAbs, bispecific antibodies (bsAb) and antibody–drug conjugates (ADC)⁵⁵, bottlenecks hampering its routine use in biopharma include (i) relatively manual experiments that require highly skilled operators

performed with nanoelectrospray capillaries of microfluidic devices and (ii) lack of automation of nIM-MS data processing.

Van der Rest et al. first demonstrated that CCS values of reference proteins obtained using SEC-nIM-MS were in good agreement with nanoESI-nIM-MS values²⁴. With therapeutic mAbs as model proteins, we compared CCS obtained with nanoESI-nIM-MS after manual desalting and SEC-nIM-MS analysis^{28, 33}. Different points should be considered when performing SEC-nIM-MS for CCS calculation. As SEC-nIM-MS experiments are performed in ESI mode, CSDs in SEC-ESI are centered on higher charge states than in nanoESI. Dipole-dipole interactions and coulombic repulsions increasing with charge state, higher charge states might be more activated, which might result in slight protein unfolding. As shown in figure 4A, similar IM calibration equations were obtained for CCS measurements performed in SEC-nIM-MS and offline injections of manually desalted proteins. Keeping that in mind, CCS were measured for a series of mAbs and show good correlation with CCS measured in nanoESI-nIM-MS (Figure 4B). In this context, SEC-nIM-MS appears as an attractive setup to automate sample preparation while widening the information content available in a single few-minutes experiment as illustrated by Ekhkirch et al. for the characterization of different therapeutic mAbs formats, including IgGs, ADCs and bsAbs²⁸. Additionally, SEC-nIM-MS affords further characterization of HMWS in stressed mAbs samples, revealing a significant conformational compaction upon mAb aggregation²⁴. Altogether, our results highlight that online coupling of SEC to nIM-MS does not significantly influence the global conformation of mAbs, which of course needs to be checked for other types of proteins.

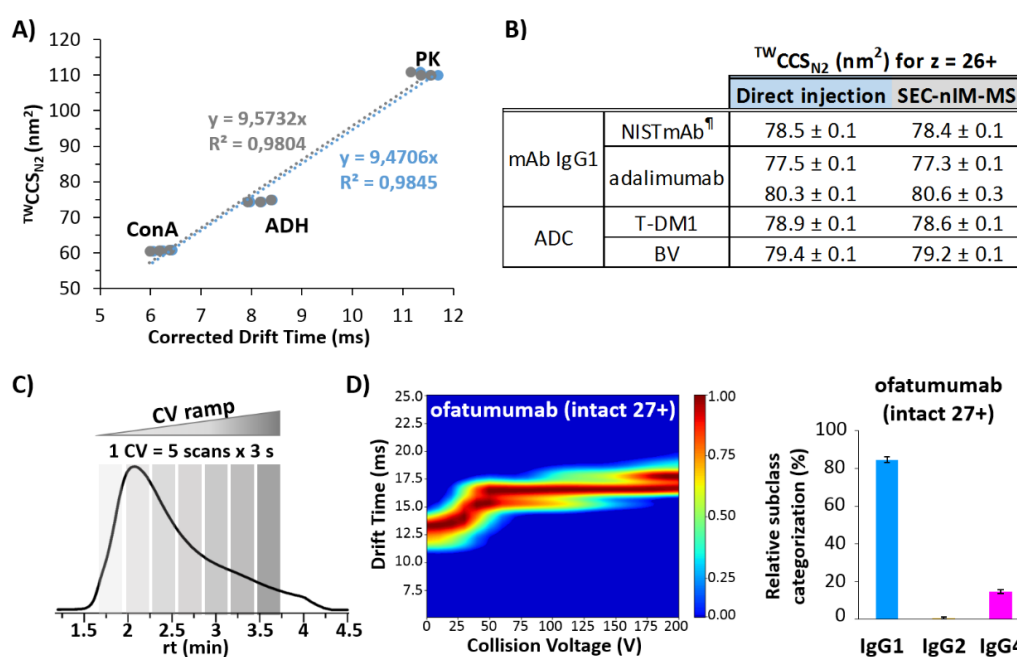


Figure 4. SEC-nIM-MS experiments for CCS measurements and CIU approaches. (A) Calibration curves for SEC-nIM-MS (grey) and offline injection (blue). ConA, ADH and PK were used as external calibrants as reported by Bush et al.⁵⁶. (B) Table summarizing CCS measurements at intact level obtained with direct nanoESI versus SEC injections. [†]All products were deglycosylated except for NISTmAb. (C) Schematic representation of SEC-CIU acquisitions. (D) SEC-CIU fingerprint and subclass classification obtained for intact ofatumumab.

SEC coupled to Collision-Induced Unfolding – CIU is an ion mobility-based approach used to probe ion gas-phase unfolding. In travelling-wave IM spectrometry (TWIMS) instruments, CIU experiments are performed by raising collision voltages (CVs) in the trap cell before IM separation, subsequently activating ions that can undergo conformational changes⁵⁷. While CIU appears as an elegant alternative

to circumvent low IM resolution of linear TWIMS cells, lack of CIU automation in both buffer exchange and data acquisition has precluded its wide adoption. In order to fully automate CIU experiments from sample preparation to data interpretation, we have developed a fast-online SEC-CIU coupling using short SEC columns, where CVs are automatically raised along sample elution (Figure 4C)³³. CIU fingerprints are generated with the CIUSuite 2 software to better visualize ATDs variations corresponding to conformational transitions (Figure 4D). This SEC-CIU setup is particularly interesting to rapidly distinguish mAbs subclasses, as the latter exhibit different unfolding patterns at both intact⁵⁸ and middle⁵⁹ levels. Diagnostic CVs regions allow to identify mAbs subclasses with scores > 80 % (Figure 4D). Targeted scheduled SEC-CIU, that is, acquisition of solely the most diagnostic CVs, helps to further reduce the data collection time while retaining clear-cut mAbs classifications.

Altogether, the combination of improved high-throughput desalting and automated data collection afforded by SEC drastically shortens the overall time process of CIU experiments, from 3 hours for classical CIU experiments with manual buffer exchange to 15 minutes for targeted scheduled SEC-CIU.

4. Hyphenation of non-denaturing LC through a SEC-based multidimensional methodology

SEC can be used for two main purposes: (i) separation and relative quantification of protein oligomers, (ii) to perform online buffer exchange prior to the analysis of proteins by nMS. However, as a consequence of the latter functionality, SEC can pave the way to allow the hyphenation of non-denaturing LC with native MS.

Coupling HIC to nMS: Development of HICxSEC-nMS strategy – Hydrophobic interaction chromatography (HIC) is the reference technique in quality control laboratories to separate and quantify the different drug-antibody ratio (DAR) populations of ADCs^{60, 61}, especially in the case of cysteine-linked ADCs for which maintaining noncovalent interactions is critical for the analysis of the whole ADC scaffold. However, the analysis of the different populations of highly heterogeneous ADCs can lead to ambiguous interpretations when this analysis is based solely on the HIC dimension. To this end, nMS can afford additional information through the mass measurement of the intact species in their native state to enable the identification of the DAR populations. Since conventional HIC solvents are not compatible with nMS, several approaches have been proposed in the literature allowing the straight hyphenation of HIC with nMS. According to the main drawbacks associated with this coupling, the different experimental strategies were based on the modification of the composition of HIC mobile phase⁶², the adoption of new HIC stationary phase materials⁶³ or the addition of a makeup flow followed by a splitting flow⁶⁴. However, these strategies require the use of nMS-compatible mobile phases, that is, ammonium acetate, along with the addition of organic modifiers, which leads to the reduction of the peak separation and the potential denaturation of proteins. To this end, Etkirch et al. designed and adapted a 2D LC system where the SEC cartridge (AdvanceBio SEC, 4.6 x 50 mm, 2.7 μ m, 300 Å) is implemented within the interface of the HIC-MS coupling enabling online buffer exchange in the front end of the mass spectrometer⁶⁵ (Figure 5A). This experimental setup was used to characterize the different populations of a conjugated mAb (Figure 5B). In this case, only five ADC populations were expected (D0, D2, D4, D6, and D8), however one additional peak is observed at 40 min in the HIC profile (Figure 5B). The mass measurement enables the assignment of the additional HIC feature as a DAR4 positional isomer (Figure 5C). The all-in-one combination of HICxSEC-nMS provided a comprehensive and streamlined characterization of all the species observed within the first LC dimension without compromising neither the chromatography separation nor the native structure of the proteins.

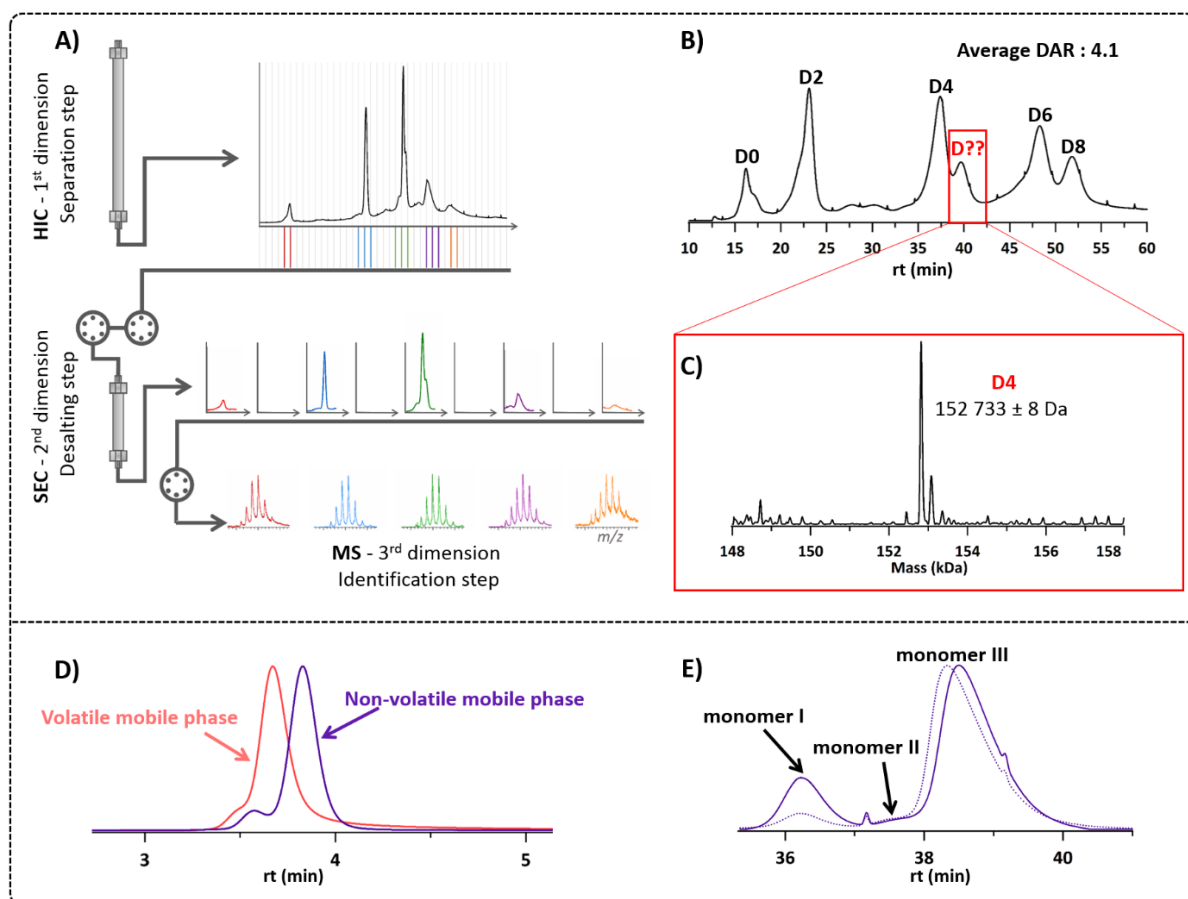


Figure 5. 2D HICxSEC-nMS and SECxSEC-nMS experiments. (A) HICxSEC-nMS setup. (B) HIC profile of an in-house investigational ADC. (C) Deconvoluted mass of the highlighted HIC peak. (D) SEC profile of intact pembrolizumab with non-volatile and volatile salts in the mobile phase. (E) Comparison of SEC profile of intact pembrolizumab (solid line) and thermal-stressed pembrolizumab (dotted line).

2D SECxSEC-nMS setup for improved SEC performances – The first non-denaturing HICxSEC-nMS setup can be considered as the basis for the conception of new MS-based multidimensional LC coupling strategies⁶⁵. The idea is to benefit from synergic effects of performing first dimension non-denaturing LC without compromising chromatographic performances while being compatible with nMS. The implementation of SEC for fast desalting between the first analytical dimension of separation and the mass spectrometer has thus a great potential to overcome the limitations of these techniques when used as standalone methods. Indeed, SEC-UV is usually performed with high concentration of non-volatile salts (typically around 100 – 500 mM) to reduce the non-specific interactions between the stationary phase and the size variant species⁶⁶. When SEC is coupled to nMS and hence, classical SEC mobile phase is replaced by MS-compatible solvents, proteins may undergo more interaction with the stationary phase (ionic and hydrophobic interactions), especially those with a pI greater than 7.0, giving rise to broader peaks with larger retention times, and leading to an underestimation of the relative intensity of size variants³⁶. This is illustrated by the example of accurate characterization of HMWS and LMWS in case of the therapeutic mAb pembrolizumab (Figure 5D). Ehkirch et al. thus developed an experimental setup based on comprehensive 2D SECxSEC coupled to nMS to determine HMWS and LMWS of non-stressed and thermal-stressed mAbs⁶⁷. The particular case of pembrolizumab pinpoints that the use of phosphate buffer in the first SEC dimension and the online combination of nMS are essential to provide baseline chromatography resolution and unambiguously assign mAb populations,

respectively (Figure 5D-E). The co-elution of the two chromatographic peaks when performing SEC with ammonium acetate mobile phase hinders the relative quantitation of both species. Furthermore, three distributions can be observed in pembrolizumab's chromatographic profile upon thermal stress (Figure 5E), which may suggest the presence of different oligomer populations, that is, trimer, dimer, and monomer. However, nMS not only revealed that different chromatographic peaks corresponded to different types of monomeric populations (Figure 5E), but also that those monomers had different degrees of oxidation.

The results obtained with these multidimensional LCxLC-IMxMS for therapeutics analysis under non-denaturing conditions pinpoints the complementarity of these techniques to expand the capabilities of non-denaturing LC and nMS techniques. In one hand, LC dimensions allow the separation and quantification of the different mAb populations based on the apparent hydrophobicity or size. On the other hand, nMS plays a pivotal role to unravel complex or unexpected chromatographic profiles affording a precise mass measurement of each individual chromatographic distribution.

Concluding remarks

In the present study, we exemplify the use of online SEC-nMS for a broader range of biomolecules ranging from homo-oligomeric proteins to proteins with nucleic acid, but also protein-small molecule complexes or even larger assemblies up to hundreds of Da. SEC-nMS is suitable for most soluble protein-protein complexes and can also be adapted for a selected series of detergents for membrane protein analysis. Online SEC-nMS in most cases not only affords rapid improved desalting efficiency but also separation of co-eluting/overlapping species. Online nMS is quite versatile as many types of commercial columns, but also manually packed ones, and LC systems are available that can be coupled to any nMS compliant mass spectrometer. In addition, the SEC-nMS coupling provides enough sensitivity to analyze low amounts of material (1 µg) with accurate mass measurements. This increase in sensitivity could be of major interest to tackle low affinity ($K_a > 100 \mu\text{M}$) assemblies or complexes maintained by weak interactions.

SEC-nMS was also the basis for the development of more complicated multidimensional 2D LCxLC workflows in which the SEC acts as fast desalting device, allowing to achieve first dimension LC separation in optimal chromatographic conditions while being compatible with downstream nMS analysis. The combination of multidimensional LC with nMS provides a synergic effect for the comprehensive characterization of mAb-based therapeutics in one single run without limiting the technical capabilities of these techniques when used as standalone techniques.

Online SEC does not hamper further IM measurements affording conformational characterization of samples either through automated CCS measurements or even for CIU experiments. In addition, further MS/MS experiments (reported for the moment only with collision-induced dissociation (CID) fragmentation) are possible. We expect ultraviolet photodissociation (UVPD) and electron-transfer dissociation (ETD) being possible also, opening the way for automatic top-down nMS.

Conflicts of interest

The authors declare no competing financial interest.

Acknowledgments

This work was supported by the CNRS, the University of Strasbourg and its IdeX program, the "Agence Nationale de la Recherche" (ANR grants ANR-16-CE11-0032 and ANR-19-CE11-0010), the French Proteomic Infrastructure (ProFI; ANR-10-INBS-08-03) and the Medalis LabEx. The authors would like to

thank GIS IBISA and Région Alsace for financial support in purchasing a Synapt G2 HDMS instrument. E.D., A.E and T.B. acknowledge the French Ministry for Education and Research, the “Association Nationale de la Recherche et de la Technologie” (ANRT) and Syndivia, and the Institut de Recherches Internationales Servier, for funding of their PhD, respectively. M. B. was supported by a fellowship from the Région Alsace.

The authors would like to thank their collaborators for kindly providing samples: Isabelle Billas Massobrio (RXR/NR7/DNA complexes) and Jean Cavarelli (PRMT2) from the IGBMC (Strasbourg, France), Alain Wagner (mAb-oligonucleotide complex, BFC, Strasbourg, France), Florence Vincent (P1/P2) from University of Aix-Marseille (Marseille, France), Xavier Manival (Rvb) from IMoPA (Nancy, France), Natàlia Carulla from the IECB (Bordeaux, France) and Alain Beck from the Institut de Recherche Pierre Fabre (Saint-Julien-en-Genevois, France).

References

1. Katta, V.; Chait, B. T., Observation of the heme-globin complex in native myoglobin by electrospray-ionization mass spectrometry. *J Am Chem Soc* **1991**, *113* (22), 8534-8535, <http://dx.doi.org/10.1021/ja00022a058>.
2. Ganem, B.; Li, Y. T.; Henion, J. D., Detection of noncovalent receptor-ligand complexes by mass spectrometry. *J Am Chem Soc* **1991**, *113* (16), 6294-6296, <http://dx.doi.org/10.1021/ja00016a069>.
3. Rostom, A. A.; Sunde, M.; Richardson, S. J.; Schreiber, G.; Jarvis, S.; Bateman, R.; Dobson, C. M.; Robinson, C. V., Dissection of multi-protein complexes using mass spectrometry: subunit interactions in transthyretin and retinol-binding protein complexes. *Proteins* **1998**, *Suppl 2*, 3-11, [http://dx.doi.org/10.1002/\(sici\)1097-0134\(1998\)33:2+<3::aid-prot2>3.3.co;2-8](http://dx.doi.org/10.1002/(sici)1097-0134(1998)33:2+<3::aid-prot2>3.3.co;2-8).
4. Rostom, A. A.; Robinson, C. V., Detection of the Intact GroEL Chaperonin Assembly by Mass Spectrometry. *J Am Chem Soc* **1999**, *121* (19), 4718-4719, <http://dx.doi.org/10.1021/ja990238r>.
5. Hochberg, G. K. A.; Benesch, J. L. P., Dynamical structure of α B-crystallin. *Prog Biophys Mol Biol* **2014**, *115* (1), 11-20, <http://dx.doi.org/10.1016/j.pbiomolbio.2014.03.003>.
6. Jore, M. M.; Lundgren, M.; van Duijn, E.; Bultema, J. B.; Westra, E. R.; Waghmare, S. P.; Wiedenheft, B.; Pul, Ü.; Wurm, R.; Wagner, R.; Beijer, M. R.; Barendregt, A.; Zhou, K.; Snijders, A. P. L.; Dickman, M. J.; Doudna, J. A.; Boekema, E. J.; Heck, A. J. R.; van der Oost, J.; Brouns, S. J. J., Structural basis for CRISPR RNA-guided DNA recognition by Cascade. *Nature Structural & Molecular Biology* **2011**, *18* (5), 529-536, <http://dx.doi.org/10.1038/nsmb.2019>.
7. Martinez-Rucobo, Fuensanta W.; Kohler, R.; van de Waterbeemd, M.; Heck, Albert J. R.; Hemann, M.; Herzog, F.; Stark, H.; Cramer, P., Molecular Basis of Transcription-Coupled Pre-mRNA Capping. *Mol Cell* **2015**, *58* (6), 1079-1089, <http://dx.doi.org/10.1016/j.molcel.2015.04.004>.
8. Saliou, J.-M.; Manival, X.; Tillault, A.-S.; Atmanene, C.; Bobo, C.; Branlant, C.; Van Dorselaer, A.; Charpentier, B.; Cianféroni, S., Combining native MS approaches to decipher archaeal box H/ACA ribonucleoprotein particle structure and activity. *Proteomics* **2015**, *15* (16), 2851-2861, <http://dx.doi.org/10.1002/pmic.201400529>.
9. Viet, K. K.; Wagner, A.; Schwickert, K.; Hellwig, N.; Brennich, M.; Bader, N.; Schirmeister, T.; Morgner, N.; Schindelin, H.; Hellmich, U. A., Structure of the Human TRPML2 Ion Channel Extracytosolic/Luminal Domain. *Structure* **2019**, *27* (8), 1246-1257.e5, <http://dx.doi.org/10.1016/j.str.2019.04.016>.
10. Jackson, V. A.; Mehmood, S.; Chavent, M.; Roversi, P.; Carrasquero, M.; del Toro, D.; Seyit-Bremer, G.; Ranaivoson, F. M.; Comoletti, D.; Sansom, M. S. P.; Robinson, C. V.; Klein, R.; Seiradake, E., Super-complexes of adhesion GPCRs and neural guidance receptors. *Nat Commun* **2016**, *7* (1), <http://dx.doi.org/10.1038/ncomms11184>.
11. Bechara, C.; Nöll, A.; Morgner, N.; Degiacomi, M. T.; Tampé, R.; Robinson, C. V., A subset of annular lipids is linked to the flippase activity of an ABC transporter. *Nat Chem* **2015**, *7* (3), 255-262, <http://dx.doi.org/10.1038/nchem.2172>.

12. Marcoux, J.; Wang, S. C.; Politis, A.; Reading, E.; Ma, J.; Biggin, P. C.; Zhou, M.; Tao, H.; Zhang, Q.; Chang, G.; Morgner, N.; Robinson, C. V., Mass spectrometry reveals synergistic effects of nucleotides, lipids, and drugs binding to a multidrug resistance efflux pump. *Proc Natl Acad Sci USA* **2013**, *110* (24), 9704-9709, <http://dx.doi.org/10.1073/pnas.1303888110>.
13. Gault, J.; Donlan, J. A. C.; Liko, I.; Hopper, J. T. S.; Gupta, K.; Housden, N. G.; Struwe, W. B.; Marty, M. T.; Mize, T.; Bechara, C.; Zhu, Y.; Wu, B.; Kleanthous, C.; Belov, M.; Damoc, E.; Makarov, A.; Robinson, C. V., High-resolution mass spectrometry of small molecules bound to membrane proteins. *Nat Methods* **2016**, *13* (4), 333-336, <http://dx.doi.org/10.1038/nmeth.3771>.
14. Ilag, L. L.; Videler, H.; McKay, A. R.; Sobott, F.; Fucini, P.; Nierhaus, K. H.; Robinson, C. V., Heptameric (L12)6/L10 rather than canonical pentameric complexes are found by tandem MS of intact ribosomes from thermophilic bacteria. *Proc Natl Acad Sci USA* **2005**, *102* (23), 8192-8197, <http://dx.doi.org/10.1073/pnas.0502193102>.
15. Sanglier, S.; Leize, E.; Dorsselaer, A.; Zal, F., Comparative ESI-MS study of ~2.2 MDa native hemocyanins from deep-sea and shore crabs: from protein oligomeric state to biotope. *J Am Soc Mass Spectrom* **2003**, *14* (5), 419-429, [http://dx.doi.org/10.1016/s1044-0305\(03\)00131-4](http://dx.doi.org/10.1016/s1044-0305(03)00131-4).
16. Rozen, S.; Füzesi-Levi, Maria G.; Ben-Nissan, G.; Mizrahi, L.; Gabashvili, A.; Levin, Y.; Bendor, S.; Eisenstein, M.; Sharon, M., CSNAP Is a Stoichiometric Subunit of the COP9 Signalosome. *Cell Rep* **2015**, *13* (3), 585-598, <http://dx.doi.org/10.1016/j.celrep.2015.09.021>.
17. Urnavicius, L.; Zhang, K.; Diamant, A. G.; Motz, C.; Schlager, M. A.; Yu, M.; Patel, N. A.; Robinson, C. V.; Carter, A. P., The structure of the dynactin complex and its interaction with dynein. *Science* **2015**, *347* (6229), 1441-1446, <http://dx.doi.org/10.1126/science.aaa4080>.
18. Snijder, J.; Rose, R. J.; Veessler, D.; Johnson, J. E.; Heck, A. J. R., Studying 18 MDa Virus Assemblies with Native Mass Spectrometry. *Angew Chem Int Ed* **2013**, *52* (14), 4020-4023, <http://dx.doi.org/10.1002/anie.201210197>.
19. Ruotolo, B. T.; Kevin, G.; Campuzano, I.; Sandercock, A. M.; Bateman, R. H.; Robinson, C. V., Evidence for Macromolecular Protein Rings in the Absence of Bulk Water. *Science* **2005**, *310* (5754), 1658-1661, <http://dx.doi.org/10.1126/science.1120177>.
20. Hall, Z.; Robinson, C. V., Do Charge State Signatures Guarantee Protein Conformations? *J Am Soc Mass Spectrom* **2012**, *23* (7), 1161-1168, <http://dx.doi.org/10.1007/s13361-012-0393-z>.
21. Duijn, E., Current limitations in native mass spectrometry based structural biology. *J Am Soc Mass Spectrom* **2010**, *21* (6), 971-978, <http://dx.doi.org/10.1016/j.jasms.2009.12.010>.
22. Cavanagh, J.; Benson, L. M.; Thompson, R.; Naylor, S., In-Line Desalting Mass Spectrometry for the Study of Noncovalent Biological Complexes. *Anal Chem* **2003**, *75* (14), 3281-3286, <http://dx.doi.org/10.1021/ac030182q>.
23. Waitt, G. M.; Xu, R.; Wisely, G. B.; Williams, J. D., Automated in-line gel filtration for native state mass spectrometry. *J Am Soc Mass Spectrom* **2008**, *19* (2), 239-245, <http://dx.doi.org/10.1016/j.jasms.2007.05.008>.
24. Van der Rest, G.; Halgand, F., Size Exclusion Chromatography-Ion Mobility-Mass Spectrometry Coupling: a Step Toward Structural Biology. *J Am Soc Mass Spectrom* **2017**, *28* (11), 2519-2522, <http://dx.doi.org/10.1007/s13361-017-1810-0>.
25. Muneeruddin, K.; Thomas, J. J.; Salinas, P. A.; Kaltashov, I. A., Characterization of Small Protein Aggregates and Oligomers Using Size Exclusion Chromatography with Online Detection by Native Electrospray Ionization Mass Spectrometry. *Anal Chem* **2014**, *86* (21), 10692-10699, <http://dx.doi.org/10.1021/ac502590h>.
26. VanAernum, Z. L.; Busch, F.; Jones, B. J.; Jia, M.; Chen, Z.; Boyken, S. E.; Sahasrabudde, A.; Baker, D.; Wysocki, V. H., Rapid online buffer exchange for screening of proteins, protein complexes and cell lysates by native mass spectrometry. *Nat Protoc* **2020**, *15* (3), 1132-1157, <http://dx.doi.org/10.1038/s41596-019-0281-0>.
27. Botzanowski, T.; Erb, S.; Hernandez-Alba, O.; Ehkirch, A.; Colas, O.; Wagner-Rousset, E.; Rabuka, D.; Beck, A.; Drake, P. M.; Cianferani, S., Insights from native mass spectrometry approaches for top- and middle- level characterization of site-specific antibody-drug conjugates. *mAbs* **2017**, *9* (5), 801-811, <http://dx.doi.org/10.1080/19420862.2017.1316914>.

28. Etkirch, A.; Hernandez-Alba, O.; Colas, O.; Beck, A.; Guillaume, D.; Cianferani, S., Hyphenation of size exclusion chromatography to native ion mobility mass spectrometry for the analytical characterization of therapeutic antibodies and related products. *J Chromatogr B: Anal Technol Biomed Life Sci* **2018**, *1086*, 176-183, <http://dx.doi.org/10.1016/j.jchromb.2018.04.010>.
29. Woodard, J.; Lau, H.; Latypov, R. F., Nondenaturing Size-Exclusion Chromatography-Mass Spectrometry to Measure Stress-Induced Aggregation in a Complex Mixture of Monoclonal Antibodies. *Anal Chem* **2013**, *85* (13), 6429-6436, <http://dx.doi.org/10.1021/ac401455f>.
30. Hengel, S. M.; Sanderson, R.; Valliere-Douglass, J.; Nicholas, N.; Leiske, C.; Alley, S. C., Measurement of in Vivo Drug Load Distribution of Cysteine-Linked Antibody-Drug Conjugates Using Microscale Liquid Chromatography Mass Spectrometry. *Anal Chem* **2014**, *86* (7), 3420-3425, <http://dx.doi.org/10.1021/ac403860c>.
31. Haberger, M.; Leiss, M.; Heidenreich, A.-K.; Pester, O.; Hafenmair, G.; Hook, M.; Bonnington, L.; Wegele, H.; Haindl, M.; Reusch, D.; Bulau, P., Rapid characterization of biotherapeutic proteins by size-exclusion chromatography coupled to native mass spectrometry. *mAbs* **2015**, *8* (2), 331-339, <http://dx.doi.org/10.1080/19420862.2015.1122150>.
32. Jones, J.; Pack, L.; Hunter, J. H.; Valliere-Douglass, J. F., Native size-exclusion chromatography-mass spectrometry: suitability for antibody-drug conjugate drug-to-antibody ratio quantitation across a range of chemotypes and drug-loading levels. *mAbs* **2019**, *12* (1), 1682895, <http://dx.doi.org/10.1080/19420862.2019.1682895>.
33. Deslignière, E.; Etkirch, A.; Botzanowski, T.; Beck, A.; Hernandez-Alba, O.; Cianféroni, S., Toward Automation of Collision-Induced Unfolding Experiments through Online Size Exclusion Chromatography Coupled to Native Mass Spectrometry. *Anal Chem* **2020**, *92* (19), 12900-12908, <http://dx.doi.org/10.1021/acs.analchem.0c01426>.
34. Goyon, A.; Beck, A.; Colas, O.; Sandra, K.; Guillaume, D.; Fekete, S., Evaluation of size exclusion chromatography columns packed with sub-3 μm particles for the analysis of biopharmaceutical proteins. *J Chromatogr A* **2017**, *1498*, 80-89, <http://dx.doi.org/10.1016/j.chroma.2016.11.056>.
35. Ventouri, I. K.; Malheiro, D. B. A.; Voeten, R. L. C.; Kok, S.; Honing, M.; Somsen, G. W.; Haselberg, R., Probing Protein Denaturation during Size-Exclusion Chromatography Using Native Mass Spectrometry. *Anal Chem* **2020**, *92* (6), 4292-4300, <http://dx.doi.org/10.1021/acs.analchem.9b04961>.
36. Goyon, A.; D'Atri, V.; Colas, O.; Fekete, S.; Beck, A.; Guillaume, D., Characterization of 30 therapeutic antibodies and related products by size exclusion chromatography: Feasibility assessment for future mass spectrometry hyphenation. *J Chromatogr B: Anal Technol Biomed Life Sci* **2017**, *1065-1066*, 35-43, <http://dx.doi.org/10.1016/j.jchromb.2017.09.027>.
37. Konermann, L., Addressing a Common Misconception: Ammonium Acetate as Neutral pH "Buffer" for Native Electrospray Mass Spectrometry. *J Am Soc Mass Spectrom* **2017**, *28* (9), 1827-1835, <http://dx.doi.org/10.1007/s13361-017-1739-3>.
38. Fekete, S.; Beck, A.; Veuthey, J.-L.; Guillaume, D., Theory and practice of size exclusion chromatography for the analysis of protein aggregates. *J Pharm Biomed Anal* **2014**, *101*, 161-173, <http://dx.doi.org/10.1016/j.jpba.2014.04.011>.
39. Vivat Hannah, V.; Atmanene, C.; Zeyer, D.; Van Dorsselaer, A.; Sanglier-Cianféroni, S., Native MS: an 'ESI, way to support structure- and fragment-based drug discovery. *Future Med Chem* **2010**, *2* (1), 35-50, <http://dx.doi.org/10.4155/fmc.09.141>.
40. Pedro, L.; Quinn, R., Native Mass Spectrometry in Fragment-Based Drug Discovery. *Molecules* **2016**, *21* (8), 984, <http://dx.doi.org/10.3390/molecules21080984>.
41. Vu, H.; Pham, N. B.; Quinn, R. J., Direct Screening of Natural Product Extracts Using Mass Spectrometry. *J Biomol Screening* **2008**, *13* (4), 265-275, <http://dx.doi.org/10.1177/1087057108315739>.
42. Ren, C.; Bailey, A. O.; VanderPorten, E.; Oh, A.; Phung, W.; Mulvihill, M. M.; Harris, S. F.; Liu, Y.; Han, G.; Sandoval, W., Quantitative Determination of Protein-Ligand Affinity by Size Exclusion Chromatography Directly Coupled to High-Resolution Native Mass Spectrometry. *Anal Chem* **2018**, *91* (1), 903-911, <http://dx.doi.org/10.1021/acs.analchem.8b03829>.

43. Maple, H. J.; Scheibner, O.; Baumert, M.; Allen, M.; Taylor, R. J.; Garlish, R. A.; Bromirski, M.; Burnley, R. J., Application of the Exactive Plus EMR for automated protein-ligand screening by non-covalent mass spectrometry. *Rapid Commun Mass Spectrom* **2014**, *28* (13), 1561-1568, <http://dx.doi.org/10.1002/rcm.6925>.
44. Jia, M.; Sen, S.; Wachnowsky, C.; Fidai, I.; Cowan, J. A.; Wysocki, V. H., Characterization of [2Fe–2S]-Cluster-Bridged Protein Complexes and Reaction Intermediates by use of Native Mass Spectrometric Methods. *Angew Chem Int Ed* **2020**, *59* (17), 6724-6728, <http://dx.doi.org/10.1002/anie.201915615>.
45. Lowe, D.; Dudgeon, K.; Rouet, R.; Schofield, P.; Jermutus, L.; Christ, D., Aggregation, stability, and formulation of human antibody therapeutics. **2011**, *84*, 41-61, <http://dx.doi.org/10.1016/b978-0-12-386483-3.00004-5>.
46. Cura, V.; Marechal, N.; Troffer-Charlier, N.; Strub, J. M.; Haren, M. J.; Martin, N. I.; Cianfèrani, S.; Bonnefond, L.; Cavarelli, J., Structural studies of protein arginine methyltransferase 2 reveal its interactions with potential substrates and inhibitors. *The FEBS Journal* **2016**, *284* (1), 77-96, <http://dx.doi.org/10.1111/febs.13953>.
47. Jeganathan, A.; Leong, V.; Zhao, L.; Huen, J.; Nano, N.; Houry, W. A.; Ortega, J., Yeast Rvb1 and Rvb2 Proteins Oligomerize As a Conformationally Variable Dodecamer with Low Frequency. *J Mol Biol* **2015**, *427* (10), 1875-1886, <http://dx.doi.org/10.1016/j.jmb.2015.01.010>.
48. Cheung, K. L. Y.; Huen, J.; Kakihara, Y.; Houry, W. A.; Ortega, J., Alternative Oligomeric States of the Yeast Rvb1/Rvb2 Complex Induced by Histidine Tags. *J Mol Biol* **2010**, *404* (3), 478-492, <http://dx.doi.org/10.1016/j.jmb.2010.10.003>.
49. Mohideen-Abdul, K.; Tazibt, K.; Bourguet, M.; Hazemann, I.; Lebars, I.; Takacs, M.; Cianfèrani, S.; Klaholz, B. P.; Moras, D.; Billas, I. M. L., Importance of the Sequence-Directed DNA Shape for Specific Binding Site Recognition by the Estrogen-Related Receptor. *Frontiers in Endocrinology* **2017**, *8*, <http://dx.doi.org/10.3389/fendo.2017.00140>.
50. Rochel, N.; Krucker, C.; Coutos-Thevenot, L.; Osz, J.; Zhang, R.; Guyon, E.; Zita, W.; Vanthong, S.; Hernandez, O. A.; Bourguet, M.; Badawy, K. A.; Dufour, F.; Peluso-Iltis, C.; Heckler-Beji, S.; Dejaegere, A.; Kamoun, A.; de Reynies, A.; Neuzillet, Y.; Rebouissou, S.; Beraud, C.; Lang, H.; Massfelder, T.; Allory, Y.; Cianferani, S.; Stote, R. H.; Radvanyi, F.; Bernard-Pierrot, I., Recurrent activating mutations of PPARgamma associated with luminal bladder tumors. *Nat Commun* **2019**, *10* (1), 253, <http://dx.doi.org/10.1038/s41467-018-08157-y>.
51. Ciudad, S.; Puig, E.; Botzanowski, T.; Meigooni, M.; Arango, A. S.; Do, J.; Mayzel, M.; Bayoumi, M.; Chaignepain, S.; Maglia, G.; Cianferani, S.; Orekhov, V.; Tajkhorshid, E.; Bardiaux, B.; Carulla, N., Aβ(1-42) tetramer and octamer structures reveal edge conductivity pores as a mechanism for membrane damage. *Nat Commun* **2020**, *11* (1), <http://dx.doi.org/10.1038/s41467-020-16566-1>.
52. Keener, J. E.; Zhang, G.; Marty, M. T., Native Mass Spectrometry of Membrane Proteins. *Anal Chem* **2020**, <http://dx.doi.org/10.1021/acs.analchem.0c04342>.
53. Leney, A. C.; Heck, A. J., Native Mass Spectrometry: What is in the Name? *J Am Soc Mass Spectrom* **2017**, *28* (1), 5-13, <http://dx.doi.org/10.1007/s13361-016-1545-3>.
54. Konijnenberg, A.; Butterer, A.; Sobott, F., Native ion mobility-mass spectrometry and related methods in structural biology. *Biochim Biophys Acta* **2013**, *1834* (6), 1239-56, <http://dx.doi.org/10.1016/j.bbapap.2012.11.013>.
55. Terral, G.; Beck, A.; Cianfèrani, S., Insights from native mass spectrometry and ion mobility-mass spectrometry for antibody and antibody-based product characterization. *J Chromatogr B: Anal Technol Biomed Life Sci* **2016**, *1032*, 79-90, <http://dx.doi.org/10.1016/j.jchromb.2016.03.044>.
56. Bush, M. F.; Hall, Z.; Giles, K.; Hoyes, J.; Robinson, C. V.; Ruotolo, B. T., Collision Cross Sections of Proteins and Their Complexes: A Calibration Framework and Database for Gas-Phase Structural Biology. *Analytical Chemistry* **2010**, *82* (22), 9557-9565, <http://dx.doi.org/10.1021/ac1022953>.

57. Dixit, S. M.; Polasky, D. A.; Ruotolo, B. T., Collision induced unfolding of isolated proteins in the gas phase: past, present, and future. *Curr Opin Chem Biol* **2018**, *42*, 93-100, <http://dx.doi.org/10.1016/j.cbpa.2017.11.010>.
58. Tian, Y.; Han, L.; Buckner, A. C.; Ruotolo, B. T., Collision Induced Unfolding of Intact Antibodies: Rapid Characterization of Disulfide Bonding Patterns, Glycosylation, and Structures. *Anal Chem* **2015**, *87* (22), 11509-15, <http://dx.doi.org/10.1021/acs.analchem.5b03291>.
59. Botzanowski, T.; Hernandez-Alba, O.; Malissard, M.; Wagner-Rousset, E.; Deslignière, E.; Colas, O.; Haeuw, J.-F.; Beck, A.; Cianférani, S., Middle level IM-MS and CIU experiments for improved therapeutic immunoglobulin subclass fingerprinting. *Anal Chem* **2020**, *92* (13), 8827-8835, <http://dx.doi.org/10.1021/acs.analchem.0c00293>.
60. Rodriguez-Aller, M.; Guillarme, D.; Beck, A.; Fekete, S., Practical method development for the separation of monoclonal antibodies and antibody-drug-conjugate species in hydrophobic interaction chromatography, part 1: optimization of the mobile phase. *J Pharm Biomed Anal* **2016**, *118*, 393-403, <http://dx.doi.org/10.1016/j.jpba.2015.11.011>.
61. Cusumano, A.; Guillarme, D.; Beck, A.; Fekete, S., Practical method development for the separation of monoclonal antibodies and antibody-drug-conjugate species in hydrophobic interaction chromatography, part 2: Optimization of the phase system. *J Pharm Biomed Anal* **2016**, *121*, 161-173, <http://dx.doi.org/10.1016/j.jpba.2016.01.037>.
62. Wei, B.; Han, G.; Tang, J.; Sandoval, W.; Zhang, Y. T., Native Hydrophobic Interaction Chromatography Hyphenated to Mass Spectrometry for Characterization of Monoclonal Antibody Minor Variants. *Anal Chem* **2019**, *91* (24), 15360-15364, <http://dx.doi.org/10.1021/acs.analchem.9b04467>.
63. Chen, B.; Peng, Y.; Valeja, S. G.; Xiu, L.; Alpert, A. J.; Ge, Y., Online Hydrophobic Interaction Chromatography–Mass Spectrometry for Top-Down Proteomics. *Anal Chem* **2016**, *88* (3), 1885-1891, <http://dx.doi.org/10.1021/acs.analchem.5b04285>.
64. Yan, Y.; Xing, T.; Wang, S.; Daly, T. J.; Li, N., Online coupling of analytical hydrophobic interaction chromatography with native mass spectrometry for the characterization of monoclonal antibodies and related products. *J Pharm Biomed Anal* **2020**, *186*, 113313, <http://dx.doi.org/10.1016/j.jpba.2020.113313>.
65. Etkirch, A.; D'Atri, V.; Rouviere, F.; Hernandez-Alba, O.; Goyon, A.; Colas, O.; Sarrut, M.; Beck, A.; Guillarme, D.; Heinisch, S.; Cianferani, S., An Online Four-Dimensional HIC×SEC-IM×MS Methodology for Proof-of-Concept Characterization of Antibody Drug Conjugates. *Anal Chem* **2018**, *90* (3), 1578-1586, <http://dx.doi.org/10.1021/acs.analchem.7b02110>.
66. Goyon, A.; Beck, A.; Veuthey, J.-L.; Guillarme, D.; Fekete, S., Comprehensive study on the effects of sodium and potassium additives in size exclusion chromatographic separations of protein biopharmaceuticals. *J Pharm Biomed Anal* **2017**, *144*, 242-251, <http://dx.doi.org/10.1016/j.jpba.2016.09.031>.
67. Etkirch, A.; Goyon, A.; Hernandez-Alba, O.; Rouviere, F.; D'Atri, V.; Dreyfus, C.; Haeuw, J. F.; Diemer, H.; Beck, A.; Heinisch, S.; Guillarme, D.; Cianferani, S., A Novel Online Four-Dimensional SEC×SEC-IM×MS Methodology for Characterization of Monoclonal Antibody Size Variants. *Anal Chem* **2018**, *90* (23), 13929-13937, <http://dx.doi.org/10.1021/acs.analchem.8b03333>.

SUPPLEMENTARY INFORMATION

Pushing the limits of native MS: Online SEC-native MS for structural biology applications

Evolène Deslignière¹, Marie Ley¹, Maxime Bourguet¹, Anthony Ehkirch¹, Thomas Botzanowski¹, Stéphane Erb¹, Oscar Hernandez-Alba¹, Sarah Cianférani^{1*}

¹Laboratoire de Spectrométrie de Masse BioOrganique, Université de Strasbourg, CNRS, IPHC UMR 7178, 67000 Strasbourg, France

*Corresponding author: Sarah Cianférani. Email: sarah.cianferani@unistra.fr

TABLE OF CONTENTS:

- **Figure S1.** SEC chromatograms obtained with different SEC columns for glycosylated trastuzumab.
- **Figure S2.** Online SEC-nMS spectra of tetrameric ADH obtained with (A) constant 250 $\mu\text{L}/\text{min}$ flowrate and (B) reduced 100 $\mu\text{L}/\text{min}$ flowrate.
- **Figure S3.** Identification and quantification of thermal-stressed trastuzumab oligomers obtained with (A) offline nMS, and (B) online SEC-nMS.
- **Figure S4.** (A) Native mass spectrum of intact pertuzumab obtained with online SEC-nMS at constant 100 $\mu\text{L}/\text{min}$ flowrate. The corresponding UV chromatogram is shown in inset. The amount of loaded mAb sample was 1 μg . (B) Variation of MS intensity of SEC-nMS as a function of injected pertuzumab sample.

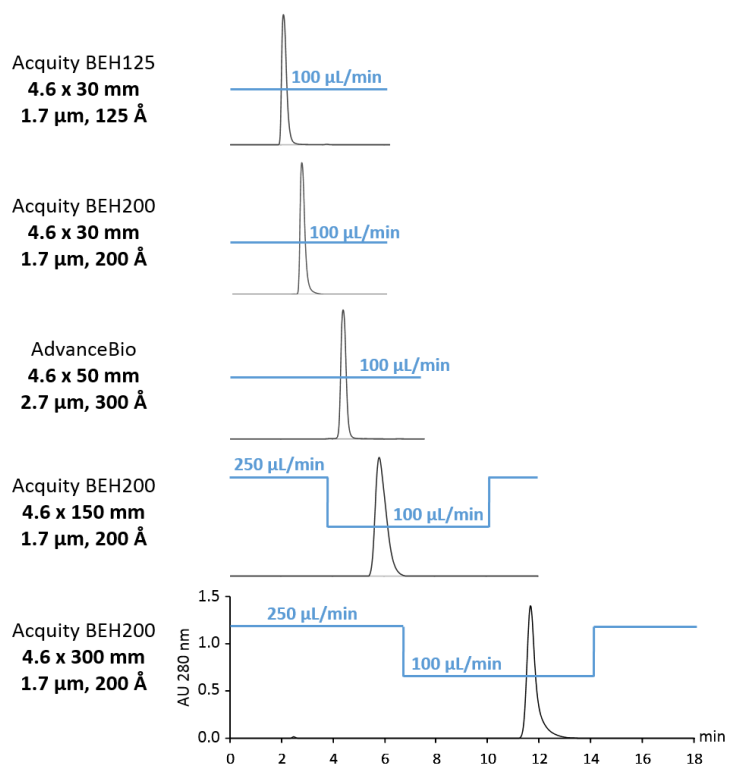


Figure S1. SEC chromatograms obtained with different SEC columns for glycosylated trastuzumab.

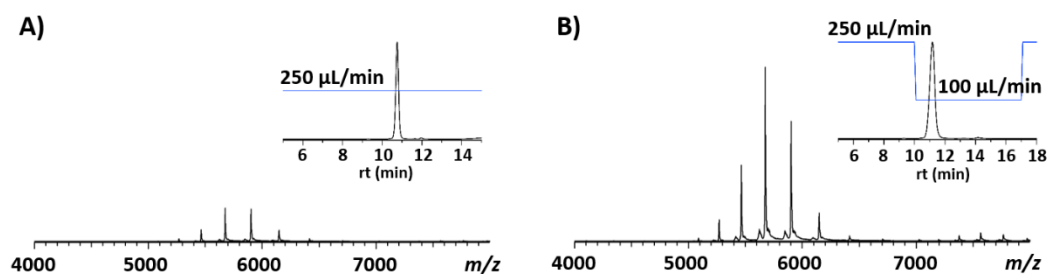


Figure S2. Online SEC-nMS spectra of tetrameric ADH obtained with (A) constant 250 $\mu\text{L}/\text{min}$ flowrate and (B) reduced 100 $\mu\text{L}/\text{min}$ flowrate.

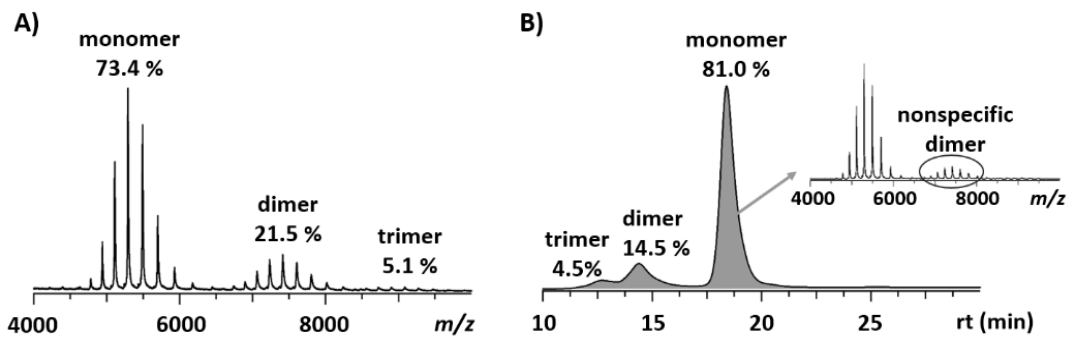


Figure S3. Identification and quantification of thermal-stressed trastuzumab oligomers obtained with (A) offline nMS, and (B) online SEC-nMS. The inset in the right-hand side of the figure corresponds to the mass spectrum of the main chromatographic peak.

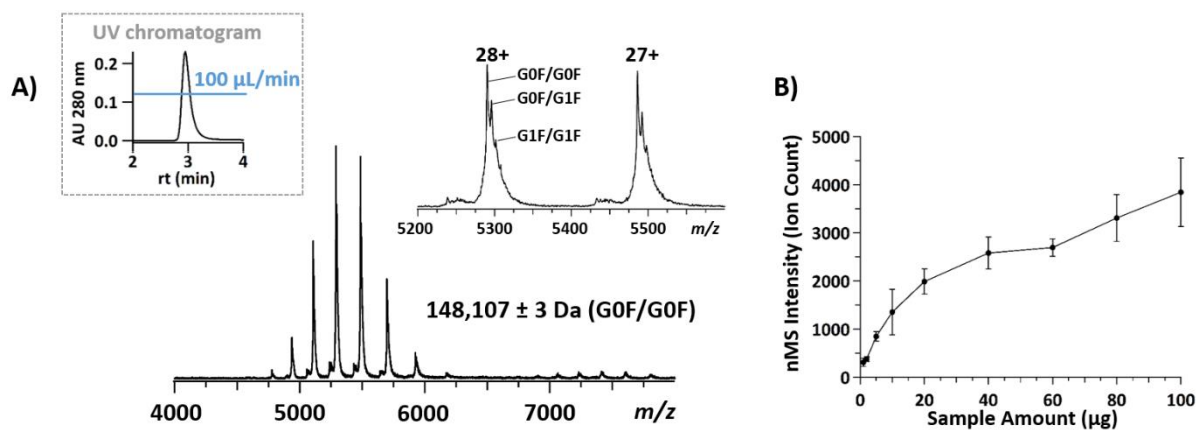


Figure S4. (A) Native mass spectrum of intact pertuzumab obtained with online SEC-nMS at constant 100 $\mu\text{L}/\text{min}$ flowrate. The corresponding UV chromatogram is shown in inset. The amount of loaded mAb sample was 1 μg . (B) Variation of MS intensity of SEC-nMS as a function of injected pertuzumab sample.